Materials Research. 2023; 26(suppl. 1):e20220589
DOI: https://doi.org/10.1590/1980-5373-MR-2022-0589

Relations of Compressive Residual Stress on Prestressed Surfaces Submitted to the Stress Shot Peening Process in EN 47 Spring Steel

Cleber Michel Chiqueti*[a] , ***Jan Vatavuk*[a]**, ***Leonardo Calicchio*[a]**, ***Rafael Cícero Penha Rocha*[b]**, ***Marcelo Pereira dos Santos*[c]**

[a]*Universidade Presbiteriana Mackenzie, Departamento de Pós Graduação da Escola de Engenharia de Materiais e Nanotecnologia, Rua da Consolação, nº 930, Bairro Higienópolis, CEP 01302-907, São Paulo, SP, Brasil.*
[b]*Universidade de São Paulo, Escola Politécnica, Departamento de Engenharia Metalúrgica e de Materiais, CEP 05508-010, São Paulo, SP, Brasil.*
[c]*Centro Universitário Fundação Santo André. Departamento de Engenharia Mecânica, CEP 09060-650, Santo André, SP, Brasil.*

Received: December 16, 2022; Revised: May 23, 2023; Accepted: May 30, 2023

This work deals with different stress shot peening conditions' effects on the compressive residual stress intensity and distribution. The tests were conducted on 15 mm x 70 mm x 1500 mm bars made of quenched and tempered EN 47 spring steel (DIN 51CrV4). Tensile tests and microstructure analysis were applied to guarantee the specification regarding resistance and microstructure. The stress shot peening process was conducted in an unloaded sample and two points bending loading with support distances of 150 and 1000 mm. The maximum flexural tension stresses were 750 and 1500 MPa for the two support distances. The residual stresses were measured by X-ray diffraction in five positions: measurements of samples with deflections were made without deflection, and a total of 95 residual stress measurements were performed before blasting. The compressive residual stresses increased as the calculated loading increased for all test conditions. Otherwise, for the 1000 mm support distance for the higher loading condition, the pre-tension calculated by the ANSYS™ showed higher flexural tension stress in the support position, while the residual stresses were constant between the supports**.**

Keywords: *Shot peening, stress shot peening, residual stress.*

1. Introduction

The blasting processes have several applications in the transformation industries, particularly in the metalworking industry, which concentrates the greatest diversity of pieces. Applications range from surface cleaning to the introduction of compressive stresses on the surface, and the shot should be a material harder than the substrate. For example, regarding surface cleaning, one can mention that the shot blast precedes steel drawing. Regarding the introduction of residual compressive stresses, the processes of shot peening, stress shot peening, warm shot peening, and laser peening[1] can be mentioned.

The process before stress shot peening is quenching and tempering, which provides mechanical properties, and then stress shot peening becomes more consistent. Clemons et al.[2] state that heat treatments significantly affect the steel's mechanical properties. In their studies, four types of steel were experimented with, which led them to obtain several mechanical properties and decarburization results. Because of that, it was known that decarburization was harmful to the life of products.

Shot peening is a blasting process of tiny particles of a material harder than the substrate that collides on the surface of this material with high speed to deform the material microscopically. This deformation mechanically causes residual compressive stresses on the material's surface due to hardening caused by impacts[3,4].

In the stress shot peening process, the same process mentioned in the shot peening process occurs with the addition of pre-tension. This pre-tension is caused by a deflection of the material, mainly where the piece will have a more mechanical solicitation. This process precedes blasting and can achieve stresses that increase the final compressive residual stress. The pre-tension is characterized by reaching stress up to the maximum of the yield strength of the material, where residual compressive stresses will be introduced on the surface, mainly using a blasting process[5]. The mechanical pre-tension process causes an instantaneous and reversible anelastic deformation, which ends up with having a higher compressive residual stress than the shot peening process since with the end of the pre-tension, the material returns to another state, which is different from the original one, since there was an amount of plasticity due to hardening work[6,7].

Nunes et al.[8] used three austenitizing temperatures (800, 850°C, and 900°C) in their experiments with AISI 4340 steel to analyze quenching parameters at navy C-rings samples.

*e-mail: cchiqueti@hotmail.com

Chiqueti[9] used AISI 5160 and AISI 6150 steel hardening temperatures of 850°C in his experiments about distortion. Their study was based on distortions with temperature variations and cooling rate agitation.

An effect of heating above austenitizing temperature is called decarburization. According to Prawoto et al.[10], decarburization refers to the diffusion of carbon from the steel to the furnace atmosphere. Therefore, a decarburized surface becomes softer due to the decreasing carbon content, and eliminating the decarburization factor is necessary to polish the surface to remove a little layer of carbon lack. Moreover, decarburization is harmful because compressive residual stress on the surface is lower than on the surface without decarburization.

The shot peening process consists of bombarding the shot at high speed[11] on the surface to increase the compressive residual stresses caused by the elastic-plastic hardening due to its shot impact. The compressive stresses are hardened in a small thickness that is less than 1 mm in quenched and tempered parts, but despite being constituted of a thin layer, they increase the fatigue life many times if that were not the case. According to Bag et al.[12], the number of cycles is increased considering the range of fatigue, loading conditions, and compressive residual stresses reached on the surface. Their experiments were made with statistical analysis, attesting to the benefit of the shot peening process. Through experiments, Korsunsky[13] discovered beneficial effects of surface peening using the determination method eigenstrain distribution with plate thickness, and, according to some parameters, it was able to predict shape deformation. Nordin and Alfredsson[14] investigated hardened SS2506 gear steel, considering peened surface coverage, and concluded that maximum compressive stresses are not dependent on intensity. The depth of maximum compressive stress increases according to increases in intensity, but it is not reliant on coverage. It is essential to point out the double shot peening process, which verified that compressive residual stress increased 10% on the surface and decreased 25 µm below the surface, and shot peening changed the topography of the surface. In the shot peening process, the part is not subjected to pre-tension, so its achieved levels of compressive residual stresses are lower than those subjected to stress shot peening. This difference is because, in the latter-mentioned process, the surface on which the blasting will take place is pre-tensioned and reaches values close to the yield strength of the material. In this way, the surface tensions are high since, in shot blasting, the density of the dislocations increases as the depth of maximum residual stress is reached. In addition to the shot peening process introducing residual compressive stresses on the surface, this process eliminates or retards the propagation of cracks, and higher-speed blasting plasticizes the material punctually through work hardening, even if this occurs at a small depth[15-17].

1.1. Compressive residual stress in depth

The depth of compressive residual stress is determined up to the point where hardening has finished. Llaneza and Belzunce[18] studied the effect of shot peening on AISI 4340 steel that was tempered and quenched at increasing temperatures for different hardness levels. The shot peening application included two conditions, referred to as SP10A and SP16A, based on the Almen intensities. The effects of these conditions on hardness and residual stress levels were separately evaluated for the different hardness levels of the ferrous matrix. As a conclusion of this study, it was found that residual stresses were higher for higher hardness levels in both shot peening conditions. In addition, the higher intensity shot peening resulted in a slight increase in the hardness depth for comparable levels. In the Figure 1 and Figure 2 are residual stress depth at two Almen intensities, using different heat treatment in steel.

The Q+T425 sample is one of AISI 4340 steel that has been tempered and quenched at a temperate of 425ºC, with a hardness of 424 HV. Concerning the other samples, sample Q+200 has a hardness of 552 HV, sample Q+T540 has a hardness of 350 HV, sample Q+T680 has a hardness of 325 HV, sample Q+T650 has a hardness of 255 HV, and sample Q+T680 has a hardness of 226 HV.

In their work, Dalaei et al.[19] concluded, by using micro-alloyed steels with 0.39%C and a hardness of 270 HV10, that surfaces treated with shot peening exhibited greater fatigue life compared to untreated surfaces. Likewise, Gundgire et at.[20] analyzed surfaces with and without shot peening and concluded that higher compressive residual stresses were observed in the shot-peened surfaces compared to those without shot peening.

Aggarwal et al.[21] investigated the fatigue life of leaf springs by varying the Almen intensity (shot peening intensity).

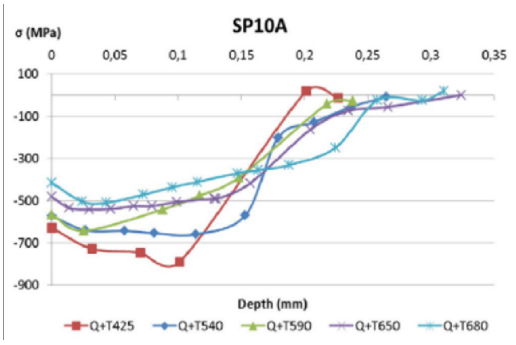

Figure 1. Residual stress profiles following different SP treatments on diverse steels. Almen intensity is 10A, full coverage.

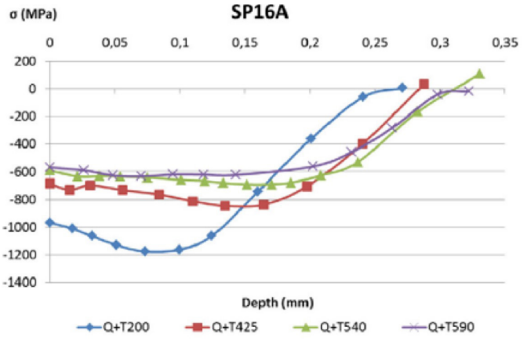

Figure 2. Residual stress profiles following different SP treatments on diverse steels. Almen intensity is 16A, full coverage.

They found that samples with higher shot peening intensity tended to have a longer fatigue life. However, the 22A shot peening intensity had a shorter fatigue life compared to 18A, which was attributed to the initiation of cracks due to defects caused by excessive peening.

Gao and Wu[22] studied the fatigue life of 7475-T7351 aluminum alloy with and without the shot peening process. They concluded that samples subjected to shot peening had reduced crack propagation rates and, consequently, increased fatigue life. This benefit was attributed to the compressive residual stresses induced by the shot peening process.

Tekeli[23] investigated the fatigue life of samples of SAE 9245 steel with and without shot peening, varying the Almen intensity. The intensities used were 10A, 15A, 20A, 25A, and 30A, with higher numbers indicating higher peening intensity. It was found that samples with shot peening intensities of 20A and 25A had an approximately 30% longer fatigue life compared to samples without the shot peening process. Samples with a 30A intensity showed a decrease in fatigue life, attributed to overpeening that can initiate cracks on the surface and remove the compressive residual stress layer.

1.2. Pre-tension

The beam deflection can be calculated according to specific criteria, such as the superposition method, direct integration method, and the use of discontinuity functions. The method used in this work is the Direct Integration Method.

Beams are narrow elements that support loads applied perpendicular to their longitudinal axis. Therefore, the beams are considered the most critical structural elements, including bars and automobile axles[24,25].

For the calculation of the elastic line, the line that is formed with the beam (in this case, bar) is supported at a symmetrical distance along the obeyed length of 1500 mm, characterizing the balance of ends at the ends, in which applied forces are located one at each end, as Figure 3 shows.

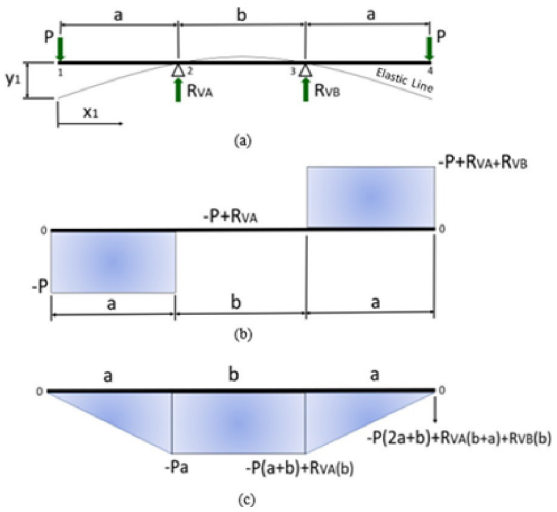

Figure 3. (a): Schematic representation of the bi-supported system with the force "P", elastic line and the distances between the supports. (b): Graph of shear force acting on the specimen. (c): Graph of moments acting on the specimen.

The characterization of the parameters is: *a* is the length of the beam (bar) from the fixed point to the first support, *b* is the length between the supports, *P* is the force applied at the ends and resulting in each support reaction, *E* is the Young modulus, *I* is the moment of inertia from the back to the center of the beam, x_1 is the length between the cantilevered end and the first support, characterized as any point included in this length, y_1 is the deformation of the elastic line between the reference line up to the deformed end, *RVA* is the support reaction on the left side of the beam, and *RVB* is the support reaction on the right side of the beam and according to the illustration in Figure 3a.

Using the equation through the Direct Integration Method, the initial formula is:

$$\frac{d^2y}{dx^2} = \frac{M}{EI} \tag{1}$$

With the development of the formula of the Direct Integration Method and its resolution, the following result of the elastic line is obtained, and the term y_1 is the theoretical deflection, which is the initial term for the calculation to determine the pre-tension.

$$y_1 = \frac{P}{6EI}\left[-x_1^3 + 3a(a+b)x_1 - a^2(2a+3b)\right] \tag{2}$$

The calculation for determining the maximum pre-tension on the tensile face of the specimen begins with the summation of the vertical forces (shear forces) and the moments in static equilibrium so that these forces and moments are equal to zero.

$$\sum F_{vertical} = 0 \tag{3}$$

$$\sum M = 0 \tag{4}$$

Conventionally, the downward force has a positive value, and the upward force has a negative value. Regarding the moment, the value is positive when the direction is clockwise, and when it is counterclockwise, the value is negative. Then, it is necessary to apply the summation equations for vertical forces and moments. The summation of the vertical forces equals zero.

Therefore, the shear force and moment graphs are represented below in Figure 3b and Figure 3c, respectively.

Thus, with the graphs of the shear force and the moments, it is possible to establish the behavior of the pre-tension that will be calculated through the Direct Integration Method, which determines the elastic line and the formula of the moment of inertia and the maximum bending tension. The formula for the moment of inertia is given:

$$I_x = \int_A y^2 dA \tag{5}$$

$$I_y = \int_A x^2 dA \tag{6}$$

The equations demonstrate the moments of inertia *Ix* and *Iy* concerning their respective axes, abscissa, and ordinate,

where *dA* is the infinitesimal element around the *x* and *y* axes, and A is the area of the figure to be calculated. Therefore, the simplified formula is:

$$I = \frac{bh^3}{12} \quad (7)$$

The Figure 4 the ordering of the axes and dimensions according to the position of the section to be calculated, making it possible to calculate the pre-tension according to the formula σ_{max}.

Therefore:

$$\sigma_{max} = \frac{Mc}{\mathrm{I}} \quad (8)$$

Where:

$_{max}$ is the maximum internal stress that occurs at the point in the cross-section of the area longer the neutral axis.

M is the resultant internal moment, determined by the method of sections and equations of equilibrium, about the neutral axis of the cross-section.

I is the moment of inertia of the cross-section calculated around the neutral axis.

c is the perpendicular distance from the neutral axis to the furthest point from the neutral axis where σ_{max} acts.

These data determine the pre-tension on the surface that will receive the blasting.

1.3. Shot peening performance

Many tests have been carried out to learn about the behavior of shot peening, and stress shot peening processes, varying parameters and thus determining the best choice for each type of process and application.

Farrahi et al.[26] concluded in their experiments that the improvement in fatigue life could be attributed to the maximum compressive residual stress and the depth of the plastically deformed layer. The shot peening process modifies the roughness of the piece, which is a function of hardness and shot size. However, hardness has the primary effect on this requirement. They showed that the compressive residual stress and the micro deformation decrease according to the applied stress and the depth of the plastically deformed layer. This decrease was faster when the fatigue load was more significant, and the diffraction line presented a possible stability when the layer plastically deformed was deeper.

Aggarwal et al.[27] simulated and tested leaf springs using various shot peening intensities based on mathematical model simulations, concluding that intensity variation induces fatigue life variations. The higher the blasting intensity, the higher the fatigue life. They carried out a fatigue test with the material in receiving condition. They observed that material with a shot peening process obtained fatigue life much higher than material in receiving condition. The highest shot peening condition showed fatigue life lower than a second higher condition because of the possibility of crack initiation on the surface associated with early relaxation on compressive residual stress during fatigue.

2. Materials and Methods

2.1. Chemical composition, tensile test, and samples dimensions

The present study measures the residual stresses on the tensile surface in EN 47 spring steel (DIN 51CrV4) samples that have the following chemical composition, according to Table 1:

The size of the samples is 15 mm in thickness, 70 mm in width, and 1500 mm in length, with a concave radius concerning the blasting surface of 2500 mm. The steel is quenched, tempered, and polished on the blasting surface to eliminate decarburization, in which the microstructure is tempered martensite.

The samples destined for the tensile test are composed of two removed and machined specimens in the sample flexion directions, according to ABNT NBR ISO 6892-1:2013 - Metallic Materials - Tensile Test, Part 1: Method and Test at Room Temperature[28]. The deformation is 0.2% for determination of Yield Strength at room temperature, using a tensile machine Wolpert/Amsler of 60 t capacity and an electronic extensometer. The Figure 5 shows the specimen,

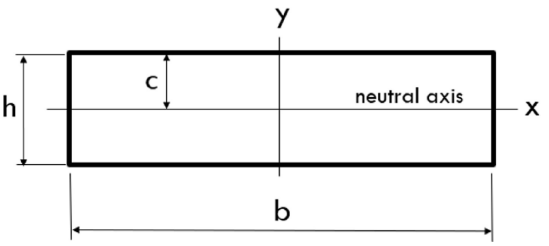

Figure 4. Cross Section and coordinates for calculating maximum tension and inertial moment, where *h* is 15 mm, *b* is 70 mm, and *c* is 7.5 mm.

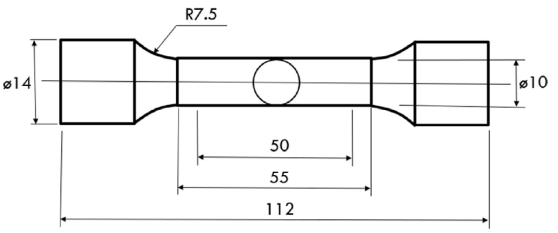

Figure 5. Specimen tensile test.

Table 1. Chemical Composition of Sample – EN 47 Spring Steel.

C	Mn	Si	W	S	Cr	Ni	Mo	V	Cu
0.525%	0.96%	0.26%	0.015%	0.008%	1.07%	0.07%	0.03%	0.114%	0.125%
Sn	Al	Ti	Nb	N	B	Pb	H	Ca	Co
0.027%	0.016%	0.041%	0.025%	0.0096%	0.0007%	0.002%	0.00017%	0.0007%	0.007%

Table 2. Mechanical Properties after Quenching and Tempering of Samples – EN 47 Spring Steel.

Sample	Yield Strength	Tensile Strength	Area Reduction	Elongation	Hardness
Sample 1	1500 MPa	1640 MPa	9.5%	39.5%	47 HRC
Sample 2	1505 MPa	1647 MPa	9.1%	37.7%	48 HRC

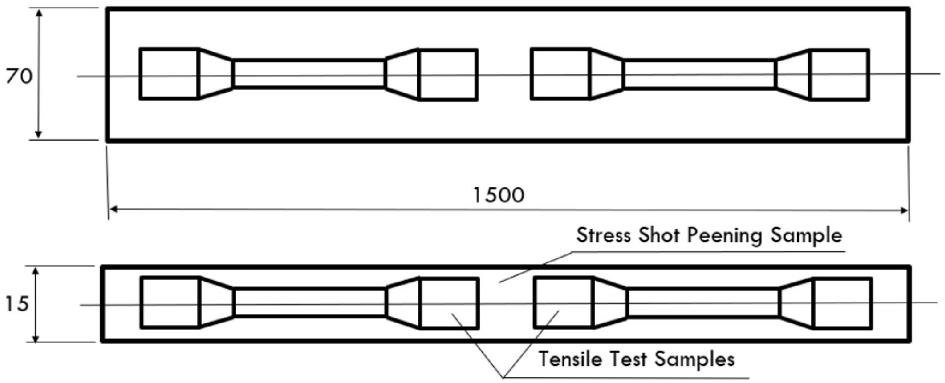

Figure 6. The design shows Stress Shot Peening and Tensile Test samples and the direction of machinery.

and Figure 6 shows the direction of the specimen submitted to the tensile test in relation to the sample.

The mechanical properties were reached after the heat treatment shown in Table 2. One stress-shot peening specimen provided two tensile test samples.

2.2. Heat treatment

The heat treatment is quenching and tempering. The quenching process is made in an industrial furnace for 25 minutes, and the temperature on the surface is 860°C before immersion in the tank with conventional and mineral oil at a temperature of 60°C. The tempering process is made in an industrial furnace for 2 hours at 430ºC. At the tank exit, there is a water shower to avoid embrittlement tempering.

2.3. Metallographic preparation

The segments of samples are cut at cutoff system trade Panambra, inlaid trade Fortel, model EFD-30, and metallographic preparation is carried out according to ASTM E3-11[29] with samples polished using polisher numbers 120, 240, 600, and 1200, as a sequence, so the last polishing is made using a diamond paste of 1 µm. Microscope Olympus BX-51M makes the metallurgical evaluation, and the pictures are recorded on camera Nikon DS-Ri1.

Reicherter durometer measures hardness in Hardness Rockwell C – HRC, loading of 150 kgf, with diamond penetrator.

The samples are free of decarburization, and the microstructure in the center of the sample is tempered martensite, according to Figure 7 and Figure 8.

The depth residual stress measurement is applied electrolytic thinning, with 10 V of electric tension, 0.7 A of electric current, and 10 µm/min thinning speed. Measurements are made in each 0.05 mm depth; then, residual stress is measured. Due to the difficulty of reading the X-ray diffraction measuring machine at specific depths, measurements ceased when the compressive residual stresses decreased.

Figure 7. Metallography shows tempered martensite microstructure without decarburization. Nital attack 2.5%.

Figure 8. Metallography shows tempered martensite microstructure in the center of the sample. Nital attack 2.5%.

2.4. X-Ray diffraction (XRD)

Residual stress measurement X-ray diffraction (XRD), trade Rigaku, model MSF-3, and testing parameters are:

Tensile constant: -299 MPa/deg.

Young's modulus: 210 GPa.

Poisson's ratio: 0.28.

Tension: 30 kV.

Current: 6 mA.

The test consists of transforming electrical energy from 380 V to 30 kV. This electric tension passes through copper cables of ø10 mm and arrives in a lamp with a filament of ø0.5 mm. Inside the lamp, acceleration is necessary for the flow of electrons to continue, but in a short space. This flux collides with a metallic Chromium wall which produces X-rays photons. These X-rays pass through a Beryllium window which stabilizes them. Then, the non-coherent emissions are filtered by a Kα filter (k alpha), and the filtered X-rays are released onto the surface to be measured.

The measurement of residual stresses is provided by X-ray diffraction for Bragg law. X-rays are trajectories of electromagnetic radiation with high energies and short wavelengths. So, when an external force deforms a metal or other polycrystalline material, it alters the crystal lattice interplanar spacing in all three dimensions and shifts the peak position of the observed diffraction profile to a greater extent, which does not happen in cases without distortion. Stress is calculated from such peak position displacements. The total width of half-maximum intensity also changes. The general Bragg equation gives the following results:

$$2d\,sin\theta = n\lambda \tag{9}$$

where d is the distortionless lattice spacing, θ the diffraction angle, n the number of wavelengths, and λ a beam of wavelength X-rays. The variable $n\lambda$ can be calculated using the equation:

$$n\lambda = d_{hkl}\,sin\phi + d_{hkl}\,sin\phi = 2\,d_{hkl}\,sin\phi \tag{10}$$

where d_{hkl} refers to the interplanar spacing from Miller indices[30,31].

In Figure 9 is X-ray diffraction representation.

The samples are fixed by the tips along their length and supported on the compressive surface with two supports, one on each side, to create a tensile pre-tension along the surface positioned upwards, which will receive the blasting and introduce compressive residual stresses. The measurement distances are fixed at -500 mm and 500 mm, corresponding to the limits of one of the sides, respectively, and 0, corresponding to the specimen's center. The measurements by X-ray diffraction, when the distance between supports is at 150 mm, are in Figure 10.

When the distance between the supports is 1000 mm, the configuration of residual stress measurement is, according to Figure 11:

The sample numbers used were 4 for each characterization in deflections (4 characterizations), 2 for characterization without deflections, and 1 for characterization after heat treatment (without the shot peening process). All measurements were made at 5 points in each sample, performing 95 XRD measurements.

The accuracy of stress measurement was $\Delta\sigma = \pm 25$ MPa.

2.5. Pre-tension calculation by ANSYS™

The deflection level at the sample tip is calculated by the principle of bent beams, using the ANSYS™ 2022, Version 2, a simulator with a mesh size of 15 mm, tetrahedral element (4 sides); also, the pre-tension applied according to the tip deflection heights are 0 MPa, 750 MPa, and 1500 MPa. 0 MPa is comprehended as a sample without deflection of the tips; and 750 MPa and 1500 MPa are comprehended as samples with maximum deflections of the tips in each characterization, according to Figures 12, 13, 14 and 15.

The Figures 12, 13, 14, and 15 show the deflections at the sample tips that cause surface pre-tensions along the surface.

2.6. Stress shot peening machine parameters

The machine is an industrial scale for blasting surfaces to increase the residual compressive stress. It comprises two turbines and boxes that are taken into a closed system for blasting. The shot used has a diameter from 0.8 to 1.0 mm with a length of 1.0 mm, and its hardness is higher than the substrate. The machine is validated through the A-type Almen strip (1.3 mm x 19 mm x 76 mm) test to verify the blasting, with the device for 4 strips, according to Figure 16, and the granulometry to verify the shot sizes; coverage is

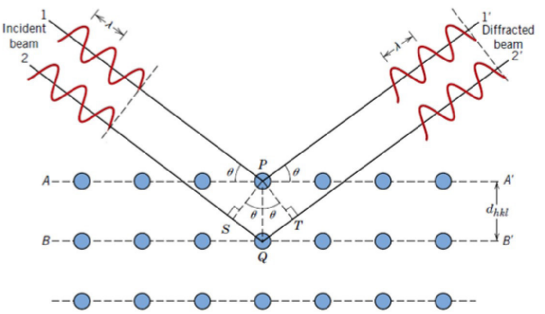

Figure 9. Schematic representation of X-ray diffraction. (Adapted from Callister and Rethwisch[30])

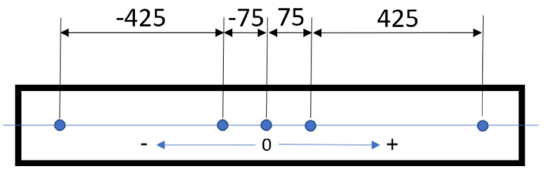

Figure 10. Measurement positions of residual stress at supports between 150 mm, on the center of the width of 70 mm.

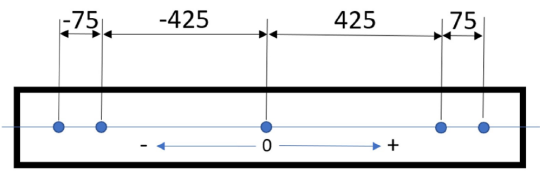

Figure 11. Measurement positions of residual stress at supports between 1000 mm, on the center of the width of 70 mm.

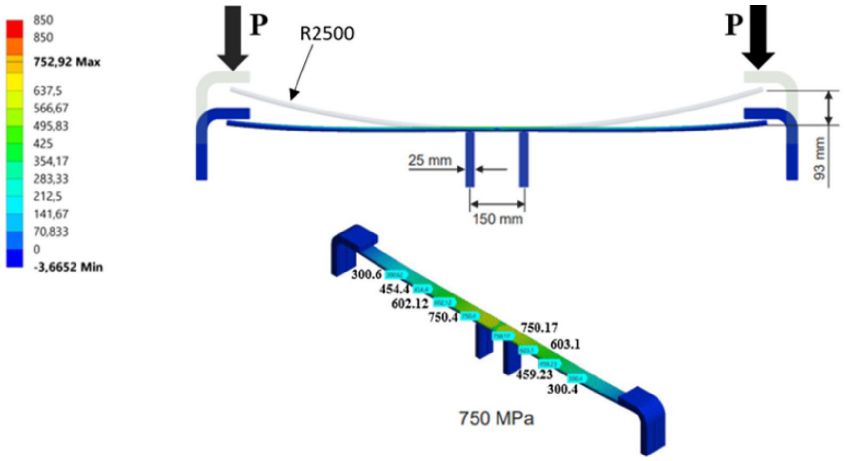

Figure 12. Calculation of maximum pre-tension of 750 MPa, pre-tension values along the surface, deflection height by finite elements is 93 mm, and distance between supports of 150 mm.

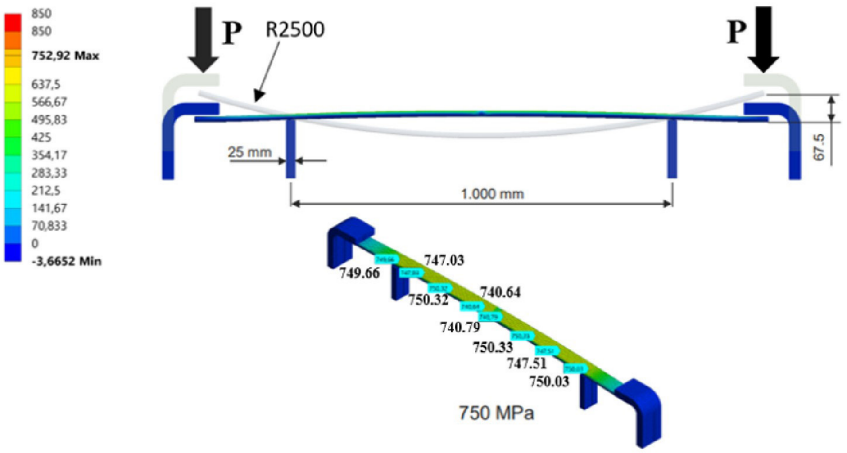

Figure 13. Calculation of maximum pre-tension of 750 MPa, pre-tension values along the surface, deflection height by finite elements is 67.5 mm, and distance between supports of 1000 mm.

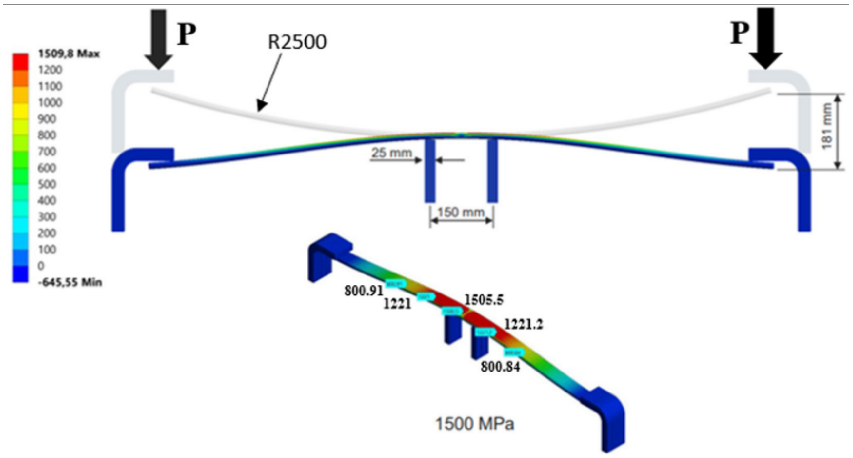

Figure 14. Calculation of maximum pre-tension of 1500 MPa, pre-tension values along the surface, deflection height by finite elements is 181 mm, and distance between supports of 150 mm.

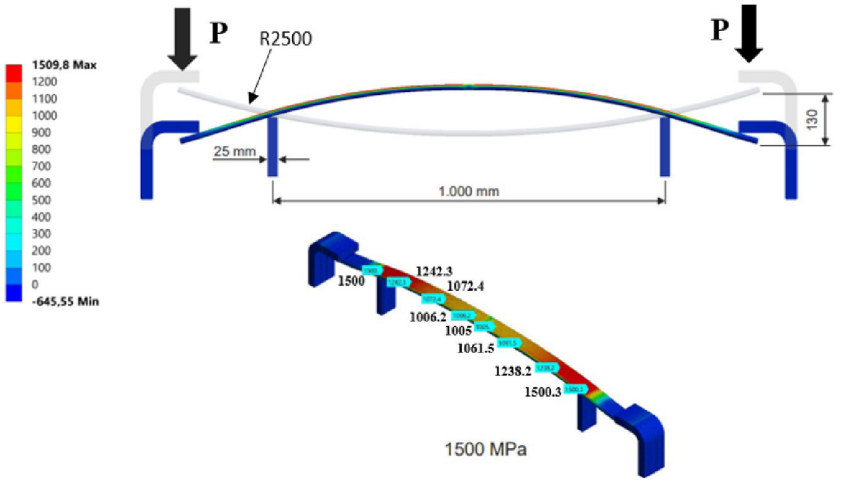

Figure 15. Calculation of maximum pre-tension of 1500 MPa, pre-tension values along the surface, deflection height by finite elements is 130 mm and distance between supports of 1000 mm.

98% minimum. Sample passage time through the turbines is 22 seconds.

The parameters were the same in all the stress shot peening machine work.

The specimen is deflected and supported by two supports on the compressive face in the convex way, according to Figure 17, with distance *d*. At the ends, two forces are applied simultaneously to deflect the sample and its fixation. First, the deflection height is calculated by the finite element system, causing a pre-tension, as shown in Figure 18. Then, the box passes through the blasting area in the longitudinal direction along its length.

The residual stress is measured by X-ray diffraction, in the longitudinal direction of the sample, which comprises the length direction (*x*-axis), according to Figure 19.

3. Results and Discussion

The austenitizing temperature used was 860°C immediately before the immersion of the sample in the tank with cooling oil. The austenitizing temperatures are cited in one work as 800°C, 850°C and 900°C[8]; and 850°C[9] in the other. The two furnaces - quenching and tempering - are of industrial scale, compatible with IATF 16949:2016[32] standard and certification.

Residual stress from heat treatment of quenching and tempering are tensile stresses caused by internal stresses induced by the microstructural change of the material. The material's microstructure passes from austenite to martensite, which occurs by changing iron allotropy from FCC (face-centered cubic) to BCT (body-centered tetragonal). Therefore, external residual stress is measured at one sample at five points equidistant from each other, and tensile residual stress in all the points are analyzed, so values are +39.83 MPa; +40.73 MPa; + 42.22 MPa; +44.74 MPa, and +47.58 MPa, which perform a medium value of +43.02 MPa (tensile residual stress).

After heat treatment was executed, samples without deflections (without pre-tension) were measured in two pieces. They were at five points in each sample, equidistant from each other. The results are in Table 3:

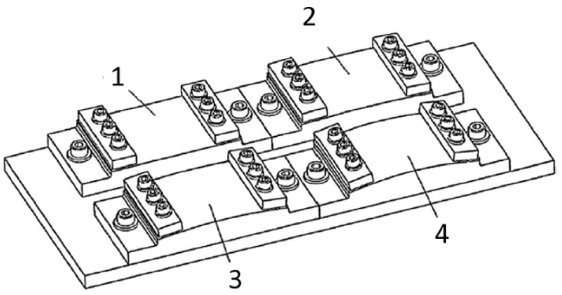

Figure 16. Device Shot Peening and Stress Shot for A-type Almen Test measurement.

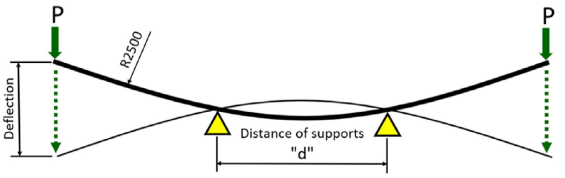

Figure 17. Illustration of sample deformation in stress shot peening process.

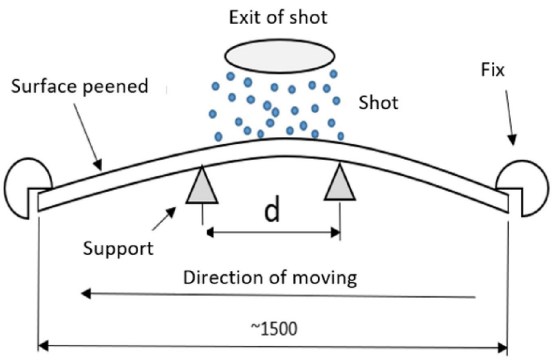

Figure 18. Illustration of stress shot peening process.

Table 3. Values of tensile residual stress, in MPa, before stress shot peening process. Pre-Tension: 0 MPa - Without Deflection.

Sample	Point 1	Point 2	Center	Point 4	Point 5	Medium Value
Sample 1	+487.91	+498.57	+502.58	+528.47	+532.45	+510.00
Sample 2	+498.73	+515.82	+537.67	-538.88	+543.76	+526.97

Table 4. Values of load theoretical calculation and pre-tension theoretical calculation, using two distances between supports and two pre-tensions.

Features	Maximum Pre-Tension (ANSYS™) 750 MPa		Maximum Pre-Tension (ANSYS™) 1500 MPa	
	d: 150 mm	d: 1000 mm	d: 150 mm	d: 1000 mm
Characterization	1	2	3	4
Deflection (ANSYS™)	93 mm	67.5 mm	181 mm	130 mm
Load Theoretical Calculation (P)	-2813 N	-7654.5 N	-5474.7 N	-14752 N
Pre-Tension Theoretical Calculation	723.3 MPa	729 MPa	1408 MPa	1404 MPa

Table 5. Values of compressive residual stress in MPa. Maximum Pre-Tension: 750 MPa – Distance between supports (d): 150 mm.

Samples	Distances of points				
	-500 mm	-75 mm	0	75 mm	500 mm
Sample 1	-612.11	-771.30	-779.55	-750.74	-615.09
Sample 2	-620.03	-764.68	-797.51	-768.34	-612.55
Sample 3	-632.20	-798.20	-806.70	-784.98	-629.84
Sample 4	-627.91	-792.74	-825.00	-791.76	-635.32
Amplitude	-20.09	-33.52	-45.45	-41.02	-22.77
Medium Value	-623.06	-781.73	-802.19	-773.96	-623.20

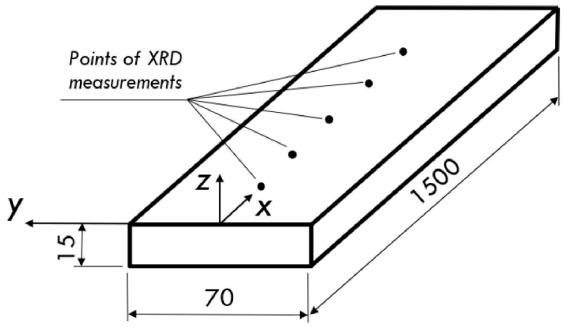

Figure 19. Positions, quantities (5 points), and direction *x* of X-Ray Diffraction (XRD) measurements.

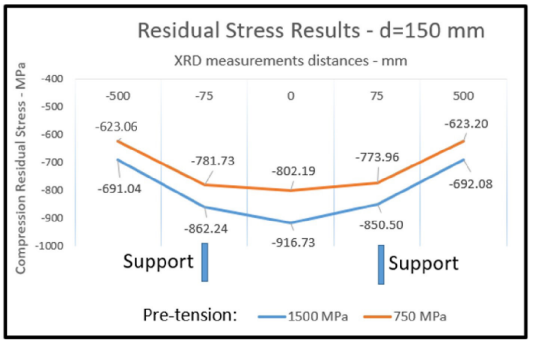

Figure 20. Results of compressive residual stress with a distance between supports of 150 mm with maximum pre-tension of 750 MPa and 1500 MPa.

The Stress Shot Peening process and the A-type Almen test used have a minimum depth of 0,020 inch for machine validation and work approval. The machine is industrial-scale compatible with IATF 16949:2016[32] standard and certification. The shot used is the same one used in the products where the experiments are conducted.

The pre-tension theoretical calculation through equations from 1 to 8 and using deflections of ANSYS™ for each characterization have the following results, according to Table 4:

The compressive residual stresses obtained in the test specimens, in which distances between the supports are 1000 mm, presented higher uniformity than the supports spaced at 150 mm. On the other hand, the highest compressive residual stresses were obtained with the supports spaced at 150 mm, according to Figures 20 and 21. Tables 5, 6, 7, and 8 present

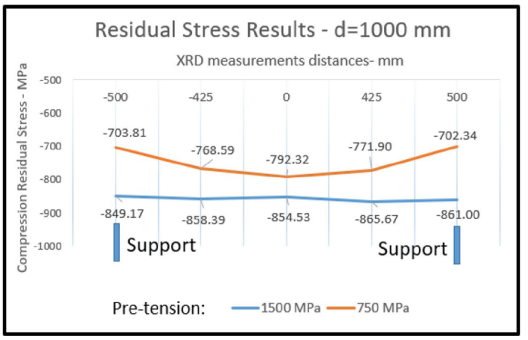

Figure 21. Results of compressive residual stress with a distance between supports of 1000 mm with maximum pre-tension of 750 MPa and 1500 MPa.

Table 6. Values of compressive residual stress in MPa. Maximum Pre-Tension: 1500 MPa – Distance between supports (d): 150 mm.

Samples	Distances of points				
	-500 mm	-75 mm	0	75 mm	500 mm
Sample 1	-673.54	-839.53	-898.39	-826.65	-672.70
Sample 2	-693.98	-862.62	-910.71	-841.18	-685.71
Sample 3	-686.88	-862.76	-922.85	-868.42	-713.06
Sample 4	-709.74	-884.06	-934.97	-865.75	-696.84
Amplitude	-36.20	-44.53	-36.58	-41.77	-40.36
Medium Value	-691.04	-862.24	-916.73	-850.50	-692.08

Table 7. Values of compressive residual stress in MPa. Maximum Pre-Tension: 750 MPa – Distance between supports (d): 1000 mm.

Samples	Distances of points				
	-500 mm	-425 mm	0	425 mm	500 mm
Sample 1	-682.70	-747.30	-771.96	-749.82	-681.62
Sample 2	-694.74	-759.24	-785.36	-776.20	-697.42
Sample 3	-723.22	-789.88	-800.37	-766.89	-706.14
Sample 4	-714.57	-777.95	-811.57	-794.67	-724.19
Amplitude	-40.52	-42.58	-39.61	-44.85	-42.57
Medium Value	-703.81	-768.59	-792.32	-771.90	-702.34

Table 8. Values of compressive residual stress in MPa. Maximum Pre-Tension: 1500 MPa – Distance between supports (d): 1000 mm.

Samples	Distances of points				
	-500 mm	-425 mm	0	425 mm	500 mm
Sample 1	-829.33	-842.13	-831.79	-848.73	-845.18
Sample 2	-840.67	-839.54	-843.21	-856.80	-850.63
Sample 3	-852.63	-869.14	-864.12	-870.59	-868.10
Sample 4	-874.03	-882.74	-878.98	-886.54	-880.09
Amplitude	-44.70	-43.20	-47.19	-37.81	-34.19
Medium Value	-849.17	-858.39	-854.53	-865.67	-861.00

the results of four samples measured by XRD, and each characterization contains amplitudes and medium values.

The ANSYS™ software (finite element analysis - FEA) presented a particularity close to the region of the supports in the characterization of the maximum pre-tension of 1500 MPa, with supports at 1000 mm. The maximum pre-tension is shown with 1500 MPa close to supports and along of sample center show 1000 MPa values, approximately (Figure 15), i.e. there is a difference about 500 MPa of pre-tension. However, the theoretical calculations (Table 4), using equations from 1 to 8 and deflection of 130 mm (Figure 15), presented maximum and constant value of 1404 MPa between supports; this constancy is referenced in Figure 3c - moment graph - where the supports have nomenclatures of RVA and RVB.

Compressive residual stress and its profile in depth are presented in Figure 22. First, the maximum depth reaches 0.25 mm with maximum compressive residual stress of -1121.68 MPa. After this depth, residual stress begins to increase. Finally, according to graph line tendency, tensile residual stress will appear.

The highest value of compressive residual stress is 0.25 mm from the surface, showing that hardening work is maximum at this point. Deepening measurement, compressive residual stress decreases. Several factors are essential for compressive residual stresses shot type and size, percentage of coverage, speed blasting, hardness of sample, and deflexion[33-36].

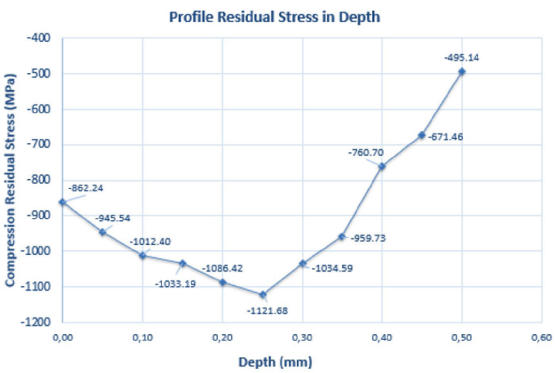

Figure 22. Compressive residual stresses in depth.

The characterization of residual stress in depth is from one point of maximum pre-tension of 1500 MPa and 150 mm between supports.

The DBL 9020:2008 Daimler AG standard[37] was used as a reference for compressive residual stress results.

4. Conclusion

The theoretical calculations compared to ANSYS™ calculation validated pre-tension established to experiments

and were at 7% maximum error considering the center point of length (750 mm), except for characterization of maximum pre-tension of 1500 MPa and 1000 mm between supports.

The characterization pre-tension of 1500 MPa and distances between supports of 1000 mm shows higher pre-tension next to supports reaching 1500 MPa. As there is advance to the center, pre-tension decreases to about 1000 MPa. The compressive residual stress line between supports is almost plane, with minimum and maximum values of -849.17 MPa and – 865.67 MPa, respectively. Therefore, this characterization's compressive residual stress distribution is unlike the pre-tension distributions calculated by the ANSYS™ software.

The difference in compressive residual stresses in the characterization of 750 MPa and 1000 mm distance between supports was almost 100 MPa. Even so, the linear distribution maintenance of pre-tension vs. compressive residual stress could be considered here.

The compressive residual stresses on the supports 150 mm apart show a profile like the pre-tension calculated by ANSYS™ (FEA), with more minor residual stresses at the ends and higher ones near the center and the supports due to the bending that induces the sample to close to its limits of mechanical properties. In comparison, the maximum pre-tension of 750 MPa and 1500 MPa values and the maximum difference between the residual stresses in the center is -114.54 MPa. Moreover, it is -67.98 MPa at a distance of -500 mm and -68.88 MPa at a distance of 500 mm. The results may show that the saturation of the material will not have a significant increase in compressive residual stress even with an increase in blasting intensity, for pre-tension of 1500 MPa.

The compressive residual stresses in the characterization with supports at a distance of 150 mm showed low values close to the compressive residual stresses of the samples that had no deflection.

The compressive residual stress distribution compared with the calculations show that with the increase in pre-tension close to the material limits, the increase in residual stress is proportionally smaller, leading to the consideration of using deflection up to the yield point. After this, compressive residual stresses are not increased as the material has already reached its plastic limit.

The highest compressive residual stress occurs at a depth of 0.25 mm, with an increase of -259.44 MPa in relation to the residual surface stress. This phenomenon happens due to the maximum work hardening and interplanar deformation caused by shot impacts that are interconnected to several parameters such as shot hardness, piece hardness, impact speed, microstructure, and others.

The difference in the distributions of the compressive residual stresses at the distances of the supports of 150 mm and 1000 mm shows that in relation to the distance of 1000 mm between the supports, the compressive residual stresses are linearly distributed. On the other hand, in the distance between 150 mm between supports, the residual compressive stresses increase from the tip to the center of the sample. However, the compressive residual stress values are higher when the supports are 150 mm apart, considering the same maximum pre-tension value.

5. Acknowledgements

This work was supported by Presbyterian Mackenzie University, Post Graduation Department at the School of Engineering of Materials and Nanotechnology. Register: 72055685

6. References

1. Vatavuk J, Vendramin JC, Canale LCF. Selected metallurgical terms in the metalworking context. São Paulo: Fontenele Publishing; 2021.
2. Clemons KC, Lorraine C, Salgado G, Taylor A, Ogren J, Umin P et al. Effects of heat treatment on steels for bearing applications. J Mater Eng Perform. 2007;16(5):592-6. http://dx.doi.org/10.1007/s11665-007-9075-6.
3. He Y, Yoo KB, Ma H, Shin K. Study of austenitic stainless steel with gradient structured surface fabricated via shot peening. Mater Lett. 2018;215:187-90.
4. Nouguier-Lehon C, Zarwel M, Diviani C, Hertz D, Zahouani H, Hoc T. Surface impact analysis in shot peening process. Wear. 2012;302(1-2):1058-63.
5. Gariépy A, Miao HY, Lévesque M. Simulation of the shot peening process with variable shot diameters and impacting velocities. Adv Eng Softw. 2017;114:121-33.
6. Liu H, Wei X, Xing S, Wang L, Zhu W, Jiang C et al. Effect of stress shot peening on the residual stress field and microstructure of nanostructured Mg-8Gd-3Y alloy. J Mater Res Technol. 2021;10:74-83.
7. Liu H, Zhu W, Jiang C, Guagliano M, Xing S, Wang L et al. Microstructure evolution and residual stress distribution of nanostructured Mg-8Gd-3Y alloy induced by severe shot peening. Surf Coat Tech. 2020;404:126465.
8. Nunes MM, Silva EM, Renzettia RA, Brito TG. Analysis of quenching parameters in AISI 4340 steel by using design of experiments. Mater Res. 2018;22(1):e20180315.
9. Chiqueti CM. Distortion studies in AISI 5160 and AISI 6150 steel under variation of bath quenching temperature and agitation [dissertation]. São Carlos: Universidade de São Paulo; 2009.
10. Prawoto Y, Yajid MAM, Lee KJ. Microstructural consideration on quantitative analysis of thermal treatment: Application to decarburization of steel. J King Saud Univ Eng Sci. 2012;25(2):141-7.
11. Hong T, Ooi JY, Shaw BA. Numerical simulation to relate the shot peening parameters to the induced residual stress. Eng Fail Anal. 2008;15(8):1097-110.
12. Bag A, Delbergue D, Ajaja J, Bocher P, Lévesque M, Brochu M. Effect of different shot peening conditions on the fatigue life of 300 M steel submitted to high amplitudes. Int J Fatigue. 2020;130:105274.
13. Korsunsky AM. On the modelling of residual stresses due to surface peening using eigenstrein distributions. J Strain Anal Eng Des. 2005;40(8):817-24.
14. Nordin E, Alfredsson B. Experimental investigation of shot peening on case hardened SS2506 Gear Steel. Exp Tech. 2017;41:433-51.
15. Shen S, Atluri SN. An analytical model for shot-peening induced residual stresses. Comput Mater Contin. 2006;4(2):75-85.
16. Miao HY, Demers D, Larose S, Perron C, Lévesque M. Experimental study of shot peening and stress peen forming. J Mater Process Technol. 2010;210(15):2089-102.
17. Lai HH, Cheng HC, Lee CY, Ling CM, Wu W. Effect of shot peening time on δ / γ residual stress profiles of AISI 204 weld. J Mater Process Technol. 2020;284(57):116747.
18. Llaneza V, Belzunce FJ. Study of the effects produced by shot peening on the surface of quenched and tempered steels:

roughness, residual stresses and work hardening. Appl Surf Sci. 2015;356:475-85.
19. Dalaei K, Karlsson B, Svensson L-E. Stability of shot peening induced residual stresses and their influence on fatigue lifetime. Mater Sci Eng A. 2011;528:1008-15.
20. Gundgire T, Jokiaho T, Santa-aho S, Rautio T, Järvenpää A, Vippola M. Comparative study of additively manufactured and reference 316L stainless steel samples-effect of severe shot peening on microstructure and residual stresses. Mater Charact. 2022;191:112162.
21. Aggarwal ML, Khan RA, Agrawal VP. Investigation into the effects of shot peening on the fretting fatigue behaviour of 65Si7 spring steel leaf springs. Proc Inst Mech Eng Pt L J Mater Des Appl. 2005;219(3):139-47.
22. Gao YK, Wu XR. Experimental investigation and fatigue life prediction for 7475-T7351 aluminum alloy with and without shot peening-induced residual stresses. Acta Mater. 2011;59:3737-47.
23. Tekeli S. Enhancement of fatigue strength of SAE 9245 steel by shot peening. Mater Lett. 2002;57:604-8.
24. Hibbeler RC. Resistência dos nateriais. 5. ed. Hoboken: Pearson Publishing/Prentice Hall; 2004.
25. Beer FP, Johnston ER Jr, DeWolf JT, Mazurek DF. Mechanics of materials. 7th ed. USA: McGraw-Hill/Bookman/AMGH Publishing; 2015.
26. Farrahi GH, Lebrun JL, Couratin D. Effect of shot peening on residual stress and fatigue life of a spring steel. Fatigue Fract Eng Mater Struct. 1995;18(2):211-20.
27. Aggarwal ML, Agrawal VP, Khan RA. A stress approach for predictions of fatigue life by shot peening of EN45A spring steel. Int J Fatigue. 2006;28(12):1845-53.
28. ABNT: Associação Brasileira de Normas Técnicas. NBR ISO 6892-1:2013: materiais metálicos – ensaio de tração. Parte 1: método de ensaio à temperatura ambiente. Rio de Janeiro: ABNT; 2013.
29. ASTM: American Society for Testing and Materials. ASTM E3-11: standard practice for preparation of metallographic specimens. West Conshohocken: ASTM; 2017.
30. Callister WD Jr, Rethwisch DG. Materials science and engineering: an introduction. 9th ed. Hoboken: Wiley; 2014.
31. Prevéy PS. Current applications of X-ray diffraction residual stress measurement. In: Voot G.V., Friel J, eds. Developments in materials characterization technologies. Materials Park: ASM International; 1996. p. 103-10.
32. IATF: International Automotive Task Force. IATF 16949:2016: automotive quality management system standard. France: IATF; 2016.
33. Kumar K, Aggarwal ML. Optimization of various design paramenters for EN45A flat leaf spring. Mater Today Proc. 2017;4(2 Pt A):1829-36.
34. Torres MAS, Voorwald HJC. An evaluation of shot peening, residual stress and stress relaxation on the fatigue life of AISI 4340 steel. Int J Fatigue. 2002;24:877-86.
35. Lin Q, Liu H, Zhu C, Chen D, Zhou S. Effects of different shot peening parameters on residual stress, surface roughness and cell size. Surf Coat Tech. 2020;398:126054.
36. Bagherifard S, Fernandez-Pariente I, Ghelichi R, Guagliano M. Effect of severe shot peening on microstructure and fatigue strength of cast iron. Int J Fatigue. 2014;65:64-70.
37. PWT/Materials and Processing Engineering. DBL 9020:2008. V.0. Ready-to-install leaf springs and struts for road vehicles. Stuttgart, DE: Daimler AG; 2008.